Contents

1 Scientific, Technical, and Management Section

1.1 Baselines and Observables

We are proposing to study a probe-scale mission to extract the wealth of cosmological information contained in the spectrum and polarization of the cosmic microwave background (CMB). The starting points for our study of a future probe are two current-decade space missions, EPIC-IM and Super-PIXIE [**? ?**]. EPIC-IM was presented to the 2010 decadal panel as a candidate CMB imaging polarization space mission. [WE COULD ALSO MENTION PRISM, WHICH IS A LITTLE LIKE EPIC-IM + SUPER-PIXIE?] It was based on a 2 m aperture telescope and 11,094 bolometric transition edge sensors. PIXIE is a proposed Explorer-scale mission focused on a measurement of the spectrum of the CMB and the large-scale B-modes. Super-PIXIE envisions a scaled up, more capable version of PIXIE. Improvements in technology by the next decade will enable designing a mission that is more capable compared to both EPIC-IM and Super-PIXIE. Therefore, all quantitative predictions presented in this proposal for EPIC-IM and Super-PIXIE represent *minimum* capabilities for future similar instruments.

The best measurements of the CMB spectrum – made by COBE/FIRAS approximately 25 years ago – show that the average CMB spectrum is consistent with that of a blackbody to an accuracy of 4 parts in 10^4 [1, 2]. Distortions in this spectrum encode a wealth of new information. The distortion shapes are commonly denoted as μ- and y-types [3, 4]. The μ-distortion arises from energy release in the early Universe and can only be produced in the hot and dense environment present at redshifts $z \gtrsim 5\times10^4$. This makes μ-distortions a unique messenger from a redshift range that is inaccessible to other astrophysical probes. The y distortion is caused by energy exchange between CMB photons and free electrons through inverse Compton scattering. These are caused at lower redshifts and are sensitive to the evolution of the large scale structure of the Universe.

Thomson scattering at the surface of last scattering is the source of the polarization of the CMB. It is useful to decompose the polarization field to two modes that are independent over the full sky, E and B-modes. Together with the pattern of temperature anisotropy T, the CMB thus gives three auto- and three cross-spectra. The *Planck* satellite and larger aperture ground-based instruments measured the T spectrum to cosmic variance limit for $\ell \leq$??. Much information remains encoded in the E and B spectra, whose full exploration has just begun [5, 6**?**].

A future CMB Probe-scale mission will address the physics of the big-bang, and quantum gravity; it will measure the sum of the neutrino masses, constrain the effective number of light particle species, and the nature of dark matter; it will probe the existence of new forms of matter at the early Universe; it will give new insights on the star-formation history across cosmic times, and it will provide information about the processes that control structure formation. In addressing these questions the Probe firmly fits into NASA's strategic plan as articulated by its Strategic Goal 1 "Expand the frontiers of knowledge", and specifically Objective 1.6 "Discover how the Universe works, [and] explore how it began and evolved".

1.2 Science Objectives

1.2.1 The Primordial Universe and Cosmic Inflation

The observed temperature and E-mode polarization of the CMB require primordial inhomogeneities in the gravitational potential, providing a remarkable observational link to the dynamics of the Universe before the hot big bang era. Inflation [7, 8, 9, 10, 11], a primordial era of accelerated expansion, provides a compelling dynamical origin for the observed statistical homogeneity of the primordial perturbations on even the largest scales. But, Inflation also predicts an as yet unobserved

spectrum of primordial gravitational waves sourced directly by quantum fluctuations of the tensor component of the metric. These gravitational waves make a distinct B-mode imprint on the polarization of the CMB. Any detection of B-mode polarization, whether generated by the primordial gravitational waves of Inflation [12, 13] or by any other source of early time vector or tensor perturbations, would reveal completely new information about the primordial era. The results would provide significant constraints and consistency checks for current models or could perhaps even overturn them. A detection would have implications far beyond the difficult question of cosmological dynamics by providing evidence for a new scale of particle physics near the GUT scale. In the context of Inflation, the relationship is particularly clear: the potential energy V of the inflaton is related to the tensor-to-scalar ratio r at the peak of the spectrum by $V^{1/4} = 3.7 \times 10^{16} \, r^{1/4}$ GeV.

Figure 1 shows current data, B-modes from vacuum fluctuations of the metric during an Inflationary era for two values of r, as well as forecasts for the determination of the CMB spectra for EPIC-IM. For testing inflation, the largest scales $\ell \leq 10$ are particularly important because they reveal the presence of B-mode correlations on scales that were super-horizon at the time of recombination [14], and because the signal is strongest relative to the B-mode from lensing. A satellite is by far the most suitable platform to making the all sky observations necessary to reach the lowest ℓ's.
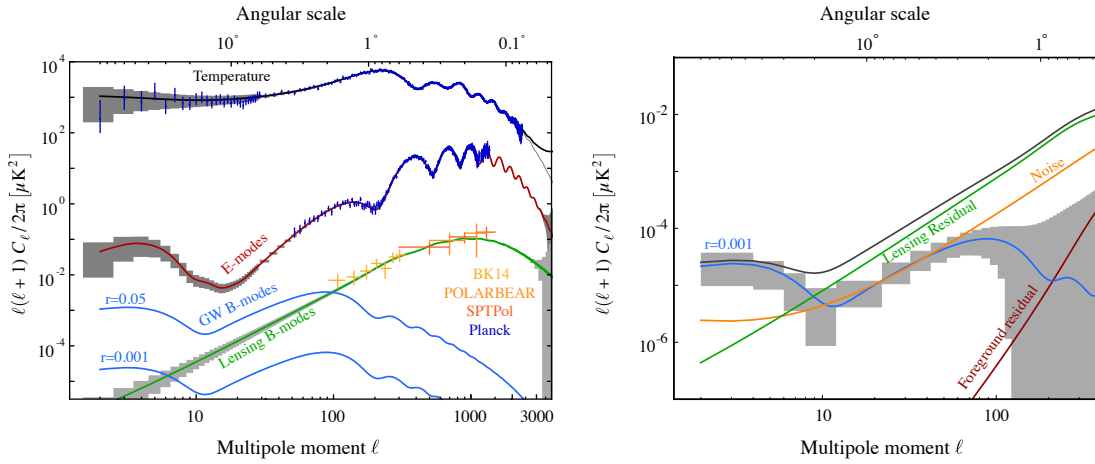

Figure 1: Predicted determination of the CMB power spectra for EPIC-IM (grey boxes) overlaid on theoretical predictions (solid lines) and including Planck measurements of the temperature and E modes (blue) and of several ground-based measurements of the lensing B-modes. The tensor B-mode predictions (blue) are shown for two representative values of the tensor-to-scalar ratio: $r = 0.001$ and $r = 0.05$.

In slow roll Inflation there are just two observationally viable classes of models that naturally explain the measured value of the spectral index n_s. One is the set of potentials $V(\phi) \propto \phi^p$, which contains many of the canonical inflation models. This set is already under significant observational pressure. If the error bars on the spectral index tighten by a factor of about 2, and the 95% C.L. upper limit on r is pushed to even ~ 0.01, all such models would be ruled out. The other class of models includes Starobinsky and Higgs inflation, which both have $r \sim 0.003$. A future mission capable of reaching $\sigma_r \sim \mathcal{O}(10^{-4})$ would provide significant constraints on nearly every currently favored inflation model. The EPIC-IM configuration is forecasted to achieve $\sigma(r) \sim 4.8 \times 10^{-4}$ assuming $r = 0.01$ and no foregrounds. **Check this statement.**

A detection of B-modes consistent with a primordial spectrum of vacuum fluctuations would be the first observation of a phenomena directly related to quantum gravity. In addition, any detection with a next generation satellite would be evidence for "large-field" inflation [15], where a

Figure 2: Forecasted constraints in the n_s–r plane for a fiducial model with $r = 0.01$ for EPIC-IM together with the current measured 1 and 2σ constraints (blue) [?]. Also shown are predictions for the models of the inflaton potential discussed in the text: Chaotic inflation for a range of $N_\star$ values (blue lines); Higgs and R^2 (large and small dots, respectively); quartic hilltop (green band); and a sub-class of α-attractor models [?]

smooth potential that supports inflation extends over a distance in field space $\Delta\phi$ of order M_p. Any inflationary model is necessarily an effective theory valid only below the scale of quantum gravity, but it is a generic expectation that additional heavy degrees (mass M) required by quantum gravity [] can easily generate structure in the low-energy potential that limits inflation to $\Delta\phi \lesssim M \sim M_p$. Studies of inflation in string theory have both born out the generic expectation [] and suggested mechanisms to realize large-field inflation []. A detection of r would therefore provide very strong motivation to better understand how large-field inflation can be naturally incorporated in quantum gravity.

Inflation generically predicts a B-mode spectrum with the shape shown in Figure 1, but inflation need not be correct [] and does not preclude additional sources of B-mode polarization either during or after inflation. To be confident of the implications of a detection, the shape and Gaussianity of the B-mode spectrum must be characterized. The vast majority of inflation scenarios predict an extremely Gaussian and very nearly scale-invariant, but slightly red, spectrum for gravitational waves. A future satellite mission, combined with Stage 3 ground based observations, could target $\sigma(n_t) \lesssim 1$ at $r = 0.01$, for example, to rule out non-vacuum inflationary sources [16, 17] and physics completely inconsistent with inflation.

Although the B-mode polarization is the richest source of new information, deeper mapping of E-mode polarization will also contribute to testing inflationary models. On the largest scales (accessible only from space), E-modes will provide new tests of isotropy, while on sufficiently small scales they will allow tighter constraints on the shape of the scalar power spectrum, the amplitude of scalar non-Gaussianities, and isocurvature modes. A satellite mission, combined with next generation ground-based instruments will improve on all measures of the scalar sector by factor of order two.

There is also much to be learned from very small scales. The dissipation of small-scale perturbations through Silk-damping [18, 19, 20, 21] leads to μ-distortions in the CMB spectrum, which provide a unique means to place stringent constraints on the amplitude of the small-scale curvature power spectrum. This information is on small scales (wavelength $0.1\,\mathrm{kpc} \lesssim \lambda \lesssim 1\,\mathrm{Mpc}$) and from early times ($10^4 \lesssim z \lesssim 10^6$), inaccessible through any other observation. In ΛCDM [21, 22], distortions are predicted at a level of $\mu = (2.0 \pm 0.14) \times 10^{-8}$ (see Fig. 3). A detection would deliver a complementary test for the inflation paradigm [23, 24, 25, 26, 27], and new probes of the particle spectrum of inflation through new tests of non-Gaussianity [28, 29, 30, 31, 32]. Precise measurements of signals at this level will be extremely challenging and requires unprecedented control of systematics and modeling of foregrounds. It would also bring us to the sensitivity level required to detect the cosmological recombination radiation [33, 34] imprinted by the recombination of hydrogen and helium at redshift $z \simeq 10^3 - 10^4$, which can be used to probe the physics
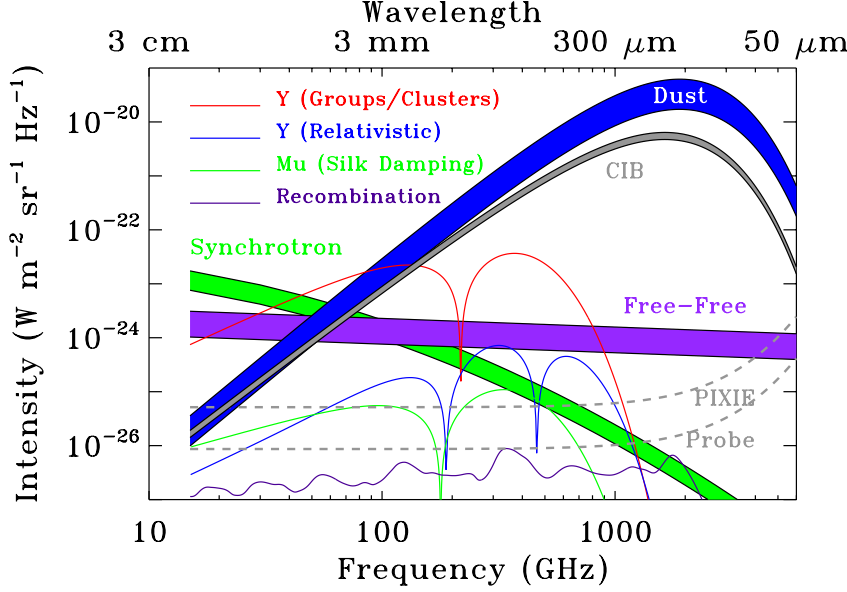
Figure 3: Main CMB spectral distortions signals and important foreground components. CMB spectroscopy could open up a new window to early-universe physics and unprecedented control of systematics and foregrounds will have to be achieved. A Probe-scale mission holds to promise for tackling all these challenges.

of recombination (see Fig. 3). Optimizing next-generation CMB spectrometers for these purposes requires extensive studies.

1.2.2 Light Relics and Dark Matter

After inflation, the universe was reheated to temperatures of at least 10 MeV and perhaps as high as 10^{10} GeV. At these high temperatures, even very weakly interacting or very massive particles, such as those arising in extensions of the Standard model of particle physics, can be produced in large abundances. As the universe expands and cools, the particles fall out of equilibrium and leave observable signatures in the CMB power spectra. Through these effects the CMB is a sensitive probe of neutrino properties and of other candidate light particles.

Much of the information about our thermal history and the particle content of the universe is encoded in the T and E power spectra. A high-precision measurement of these spectra over the full sky is expected to significantly improve our understanding of the post-inflationary universe. This is particularly true in E-mode polarization where, to date, far fewer modes have be measured at the level of cosmic variance than in temperature.

One particular compelling target is the effective number of neutrino species N_{eff}, which parameterizes the total amount of energy density in radiation at the time of recombination. Despite its common name, N_{eff} encodes the total number of light relic particles. The canonical value with three species of neutrinos is $N_{\text{eff}} = 3.046$. Additional light particles contribute a change to N_{eff} of at least $\Delta N_{\text{eff}} \geq g\,0.027$ where $g \geq 1$ is the number of degrees of freedom of the new particle [35, 36]. This defines a compelling target of $\sigma(N_{\text{eff}}) < 0.027$ for future CMB observations. New light particles are a common feature of many approaches to physics beyond the Standard model and are directly tied to some of the most significant problems in the Standard model. Either a limit or detection of ΔN_{eff} at this level would provide a powerful insight into the fundamental laws of nature.

The presence of free-streaming radiation changes the detailed features of the TT, TE and EE spectra at all ℓ. In particular, it changes the locations of the acoustic peaks and alters the damping tail at high-ℓ [37, 38, 39, 40]. Similar changes to the spectra arise from many other compelling targets including the helium fraction Y_p and more general dark sector physics. For this reason, constraints on N_{eff} a useful proxy for the information available in the high-ℓ power spectra.
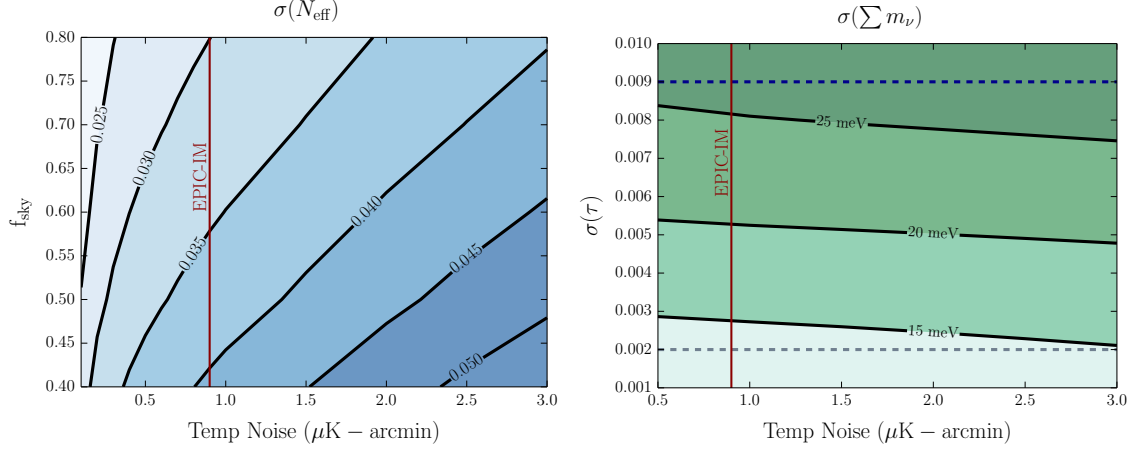
Figure 4: $N_{\rm eff}$ as a function of noise and sky fraction assuming 5' resolution (left) and Neutrino mass constraints as a function of uncertainties in measurement of τ and noise for a 5' beam and sky fraction of $f_{\rm sky} = 0.7$. Vertical lines denote the expected performance of EPIC-IM. The blue dashed line is the current *Planck* limit; the grey dashed line is the limit from cosmic variance measurement of τ. All forecasts assume internal delensing of the T and E-maps [41], including residual non-Gaussian covariances.

Forecasts for $N_{\rm eff}$ are shown in the right hand panel of Figure 4. The two most important quantities for improving constraints on $N_{\rm eff}$ and other high-ℓ targets are the fraction of sky observed $f_{\rm sky}$ and the noise temperature. Both are specific strengths of a space mission. The EPIC-IM mission reaching an effective noise temperature noise of 0.9 μK-arcmin over the full sky gives competitive constraining power when compared other proposals. The full-sky nature of the proposed mission would allow for cosmic variance limited E-modes over most of the sky and a large range of ℓ.

The main downside of a space-based mission is that we cannot reach the resolutions available from the ground. However, we see that at 5' resolution and 1 μK-arcminute noise the forecasts are less sensitive to the resolution then one might naively expected. In particular we can reach $\sigma(N_{\rm eff}) < 0.035$ for temperature noise from 1-2 μK-arcmin and $f_{\rm sky} = 0.6 - 0.8$. These forecasts are competitive with CMB Stage IV. Specifically, the larger sky fraction and sensitivity available from space appears to compensate for the reduced resolution. In fact, the full sky measurement would provide complimentary information that could be combined with ground based surveys to further improve over the limits available from either experiment. This is particularly important for $N_{\rm eff}$ which is tantalizingly close to the target of $\sigma(N_{\rm eff}) = 0.027$ and therefore even an apparently modest improvement could have a major scientific impact.

Measurements of the primary CMB and CMB lensing are very sensitive to particles with long-lifetimes that service until the era of recombination. Furthermore, the primary CMB is indirectly sensitive to BBN through the helium fraction, Y_p, that can be detect energy injections at those times. However, many relics of the early universe are not cosmologically stable but can survive beyond the time of BBN. Energy injection between the two eras is not directly captured by the CMB anisotropies but can be tested by BBN consistency of Y_p with the measured value of $N_{\rm eff}$ [40, 42].

Additional, far more sensitive measurements of this intermediate era are possible through the *distortions* of the CMB blackbody spectrum. This will allow us to place stringent bounds on the presence of long-lived decaying particles, with lifetimes $t_{\rm X} \simeq 10^6 - 10^{11}$ s [25, 43, 44, 45, 46, 47]. CMB distortion measurements could thus complement existing bounds from CMB anisotropy measurements on particles with even longer lifetimes [48, 49, 50] and improving constraints derived from light-element abundances [51, 52, 53] by more than two orders of magnitude, potentially

breaking the degeneracy between lifetime and abundance of the particle [25, 46, 54]. CMB spectroscopy is also sensitive to other non-standard physics, such as axions, primordial magnetic fields and superconducting strings [e.g., 55, 56, 57, 58, 59], providing new complementary probes of particle physics and inflation.

Through cosmological measurements, we have already confirmed the existence of one relic that lies beyond the Standard Model: dark matter. Characterizing the nature of dark matter is one of the most basic problems in cosmology and astro-particle physics. For a conventional WIMP candidate, the CMB places very stringent constraints on dark matter through possible energy injection at the time of recombination. A thermal relic will necessarily annihilate into Standard model particles which distorts the Thomson visibility function and ultimately the shape of the primary T and E spectra [48, 60, 61]. A dark matter candidate can also have a slow decay to Standard models particles which is similarly constrained by the CMB [48, 49, 50, 62].

A somewhat more model-independent approach is to constraint dark matter interactions that would effect the evolution of the effective dark matter fluid and its interactions with baryons or photons. The simplest example is to constraint the baryon-dark matter cross section through its effective coupling of the two fluids [63]. These couplings effect the evolution of fluctuations and ultimately the T and E spectra. More exotic dark sectors can produce a rich phenomenology in the CMB and in the large-scale structure without necessarily producing an associated signature in direct detection experiments or indirect searches (e.g. [64, 65, 66]).

Interactions of DM with standard model particles can also be constrained through CMB spectral distortions [67]. As the Universe expands, the matter cools. Compton interactions with electrons keep the normal matter at the CMB temperature until well after recombination. This leads to a small distortion of the CMB with a negative chemical potential [54]. In a similar manner, interactions of DM with electron, protons or directly with CMB photons can lead to a distortion. Current constraints from FIRAS are most sensitive to small DM mass, $m_{\mathrm{X}} \lesssim 0.2\,\mathrm{MeV}$, but these could be extended to $m_{\mathrm{X}} \lesssim 1\,\mathrm{GeV}$ with a Probe-class mission, testing DM interaction down to cross-sections $\sigma \simeq 10^{-39} - 10^{-35}\,\mathrm{cm}^2$ [67]. This complements and improves existing constraints [68, 69] and also opens a new avenue for testing DM-proton interactions [67].

1.2.3 Neutrino Mass

One of the last unknowns of the Standard model of particle physics is the absolute mass scale of the neutrinos. While measurements of neutrino oscillations demonstrate the neutrinos have mass, directly measuring the scale of the masses is challenging experimentally. Current measurement of N_{eff} confirm the existence of a cosmological abundance of neutrinos whose gravitational influence is detectable in the CMB and in large scale structure. Cosmology presents a unique opportunity to measure the the sum of neutrino masses $\sum m_\nu$ through the suppression of the growth of structures in the Universe on small scales. In fact, the CMB allows for an internal measurement $\sum m_\nu$ by comparing the amplitude of the lensing power spectrum to that of the other CMB spectra [70].

The CMB Probe would be a valuable tool in the quest for a cosmological detection of $\sum m_\nu$. The sensitivity to $\sum m_\nu$ from suppression of power alone is limited by our knowledge of the primordial amplitude of fluctuations A_s which is strongly degenerate with the optical depth τ. The current limit on τ from *Planck* of $\tau = 0.055 \pm 0.009$ [] limits $\sigma(\sum m_\nu) \gtrsim 25$ meV; see Figure 4. Therefore, a detection of the minimum value expected from particle physics $\sum m_\nu = 58$ meV at 3-5 σ depends crucially on an improvement measurement of τ.

To date, the only proven method for such a measurement is from a space-based CMB observations. The best constraints on τ come from E-modes with $\ell < 20$ which requires control over

the largest angular scales. The CMB Probe could, in principle, reach the cosmic variance limit of $\tau \sim 0.002$ and could reach $\sigma(\sum m_\nu) < 15$ meV when combined with DESI BAO. A detection of $\sum m_\nu$ at this level is not possible with any existing survey without an improvement to the measurement of τ.

1.2.4 Cosmological structure formation

Understanding the evolution of cosmological structures from the formation of the first stars to the present time is a key goal of cosmology [71]. [REMOVE LINE BREAK?]

In particular understanding cosmological reionization, the transformation of neutral hydrogen into an ionized state, and establishing a connection between reionization and early galaxies, will reveal valuable information about the star formation history and the physical processes that formed the galaxies of various luminosities and masses we see today. [ADD LINE BREAK?] Though a number of diverse observational probes have rendered a preliminary picture of the reionization epoch, details of the transition from the neutral to ionized Universe are still the subject of intense activity. In the current picture, early galaxies reionize hydrogen progressively throughout the entire Universe between $z = 12$ and $z = 6$, while quasars take over to reionize helium from $z \simeq 6$ to $z \simeq 2$. However many questions remain. When did the epoch of reionization (EoR) start, and how long did it last? Are early galaxies enough to reionize the entire Universe or is another source required? To answer these questions one can resort to using the traces left by the EoR in the cosmic microwave background (CMB) anisotropies. More specifically, the integrated Thomson scattering optical depth, τ, due to the scattering of CMB photons off free electrons after reionization, as inferred from the polarised CMB photons. The optical depth to reionization, τ, places an important integral constraint on the extended reionization history. The *Planck* Collaboration [? ?] reported recently a value of $\tau = 0.055 \pm 0.009$ significantly lower than previous estimates. This suggests that an early onset of reionization is strongly disfavoured by the *Planck* data. The *Planck* Collaboration [?] showed that this result reduces the tension between CMB-based analyses and constraints from other astrophysical sources. A cosmic variance limited measurement of E-mode polarization on large scales, possible with a probe mission, will render the most accurate determination of τ (Figure 4 shows a cosmic variance limit measurement of τ along with the current *Planck* limit, break the degeneracy with the neutrino mass, set stringent constraints on models of the reionization epoch, and, finally, help understanding the formation of the cosmological structures we see today.

The anisotropies in the Cosmic Infrared Background (CIB), produced by dusty star-forming galaxies (DSFGs) in a wide redshift range, are an excellent probe of both the history of star formation and the link between galaxies and dark matter across cosmic time. The *Planck* Collaboration [72, 73], derived values of the star formation rate density that, at redshifts z$\sim$ 3, are about three times higher than constraints from number counts measurements ([74]). The new mission probe, by measuring CIB anisotropies with 100 times more sensitivity than *Planck*, will be able to shed light on this intriguing discrepancy. In particular, it will be possible to constrain the global star formation rate (SFR) with one tenth of *Planck*'s uncertainty at z= 3. Moreover, it will be possible to identify and constrain a characteristic halo mass $M_{\rm eff}$, which determines the most efficient gas accretion and SFR, and therefore sets the evolution of the galaxies residing within a dark matter halo. Current models and measurements constrain this characteristic halo mass at $M_{\rm eff} \sim 10^{12}$ solar masses with about 10% uncertainty, while the new mission probe will constrain this parameter at the percent level.

Moreover, because DSFGs trace the underlying dark matter field in a broad redshift range, the CIB

will correlate with multiple dark matter tracers such as catalogs of galaxies and quasars [75, 76], and diffuse maps of the γ-ray and the X-ray background [77]. These cross-correlations will provide an additional probe of the global star formation history, and they will shed light on the interaction between light and matter in a broad wavelength range.

Large-scale structure can also be probed using CMB spectral distortions measurements. In fact, the largest guaranteed distortion is caused by the associated late-time energy release of forming structures and from reionization [78, 79, 80, 81, 82], imprinting a y-type distortion with $y \simeq 2 \times 10^{-6}$ [e.g., 82, 83]. This distortion is only one order of magnitude below the current limit from COBE/FIRAS and, even with most pessimistic assumptions about foregrounds, should be clearly detected with the next-generation spectrometers we propose to study. A detection will give information about the total energy output of first stars, AGN and galaxy clusters. In particular, group-size clusters that have masses $M \simeq 10^{13} \, M_\odot$ contribute significantly to the signal. With temperature $kT_e \simeq 1 \, \mathrm{keV}$ these are still sufficiently hot to create a detectable relativistic temperature correction to the large y-distortion, which can be used to constrain the currently uncertain feedback mechanisms used in hydrodynamical simulations of cosmic structure formation [83]. These two inevitable signals probe the low-redshift Universe and provide clear targets for future spectral distortions measurements and their requirements in the presence of foregrounds (see Fig. 3).

The CMB spectrum varies spatially across the sky. One source of such anisotropic distortion is related to clusters of galaxies and has already been measured by Planck [84]. A combination of precise CMB imaging and spectroscopic measurements will allow observing the relativistic temperature correction of individual SZ clusters [85, 86, 87], which will calibrate cluster scaling relations and inform our knowledge of the dynamical state of the cluster atmosphere. Finally, resonant scattering signals in the recombination [88, 89, 90] and post-recombination eras [91, 92] can lead to spectral-spatial CMB signals that can be used to constrain the presence of metals in the dark ages and the physics of recombination. For all these applications, instrumental synergies between CMB imaging and spectroscopy need to be studied in detail.

These studies will be key to address three of the seven key questions identified in the Astro2010 report "New Worlds, New Horizons in Astronomy and Astrophysics" (NAS Decadal Survey, p. 47): *What is the fossil record of galaxy assembly from the first stars to present? What are the connections between dark and luminous matter? How do cosmic structures form and evolve?*

1.3 The Challenges: Foregrounds, systematics

3 pages. Discuss the challenge of Foregrounds and Systematics.

The search for primordial B-modes is one of the main science objectives of any future CMB mission. A satellite mission is the most sensitive probe of this signal from the early universe because it can access the full sky and the choice of frequencies is not limited by the atmosphere.

By the time of launch of a probe class mission substantial progress will already have been made. In the case of a detection at the time of launch, the probe mission should be able to convincingly detect the expected reionization signal. In the absence of a signal it should significantly improve the upper limits beyond $\sigma(r) = 0.001$.

The contribution from reionization to the Stokes Q-parameter for a tensor-to-scalar ratio $r = 0.001$ is shown in the left panel of Figure 5. The amplitude of the signal is approximately 10 nK so that any experiment attempting to measure such a signal must control foregrounds and systematics on large angular scales at an unprecedented level of a few nK.
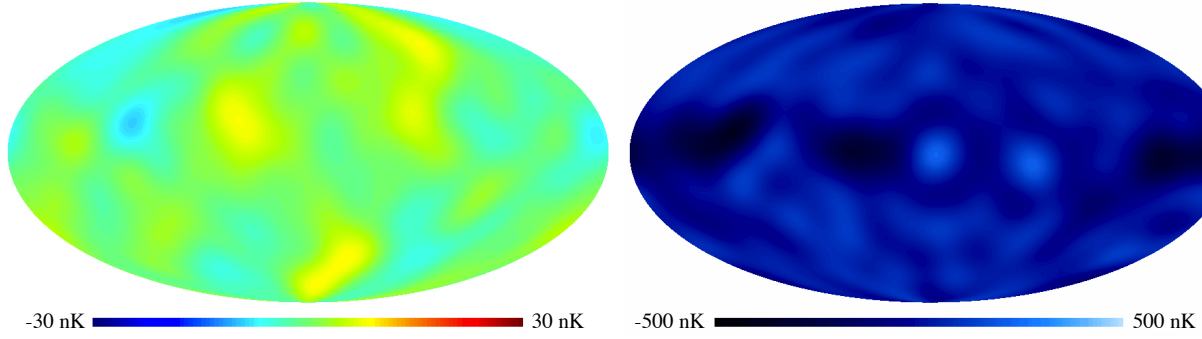
Figure 5: *Left panel:* Contribution to the Stokes Q parameter from inflationary B-modes for $\ell < 12$ for $r = 0.001$. *Right panel:* Noise in the $Planck$ 353 GHz map of the Stokes Q parameter for $\ell < 12$ rescaled to 150 GHz assuming the spectral properties of dust.

1.3.1 Foregrounds

Data from the $Planck$ satellite has significantly improved our understanding of foregrounds in both intensity and polarization. In polarization, the sky is dominated by the expected sources, synchrotron and dust, and $Planck$ has provided us with much improved measurements of their amplitude and spectral dependence. The observed spectral dependence is shown in the left panel of Figure 6 for different sky fractions. One of the most important lessons is that foregrounds are larger than putative primordial B-mode signal everywhere.

This is particularly severe on the scales relevant for the search of primordial B-modes as can be seen in the right panel of Figure 6, which shows the power spectrum of foregrounds over 75% of the sky for frequencies between 70 and 200 GHz together with the lensing and inflationary contribution for different values of the tensor-to-scalar ratio.

Perfect knowledge of the foreground components would allow to remove them, but the sensitivity of Planck limits our ability. The right panel in Figure 5 shows the noise in the $Planck$ 353 GHz map of the Stokes Q-parameter rescaled to 150 GHz assuming the same spectral dependence as for dust and on the angular scales relevant for the measurement of the inflationary B-modes. The noise is more than an order of magnitude larger than the inflationary contribution for $r = 0.001$, clearly indicating the necessity to measure foregrounds with a potential future space mission. A probe class mission likely is the only way to map foregrounds at a level required to measure primordial gravitational waves for $r < 0.001$.

While the search for primordial B-modes leads to the strictest constraints on foreground residuals, exquisit control of foregrounds is also necessary for other science objectives. A satellite mission is likely also the only reliable way to measure the optical depth at a level necessary to break the degeneracy with the neutrino mass. Furthermore, a cosmic variance limited measurement of E-mode polarization on large scales possible with a probe mission would contain valuable information about the star formation history.

Similarly, a clear objective of the spectral science is to have a robust, foreground-marginalized expectation of detecting the μ-distortion generated by the dissipation of small-scale acoustic modes in ΛCDM. While an instrument like PIXIE just falls short of this objective, it seems within reach of a probe mission.

One of the key ingredients in the design of a CMB experiment is the frequency coverage re-
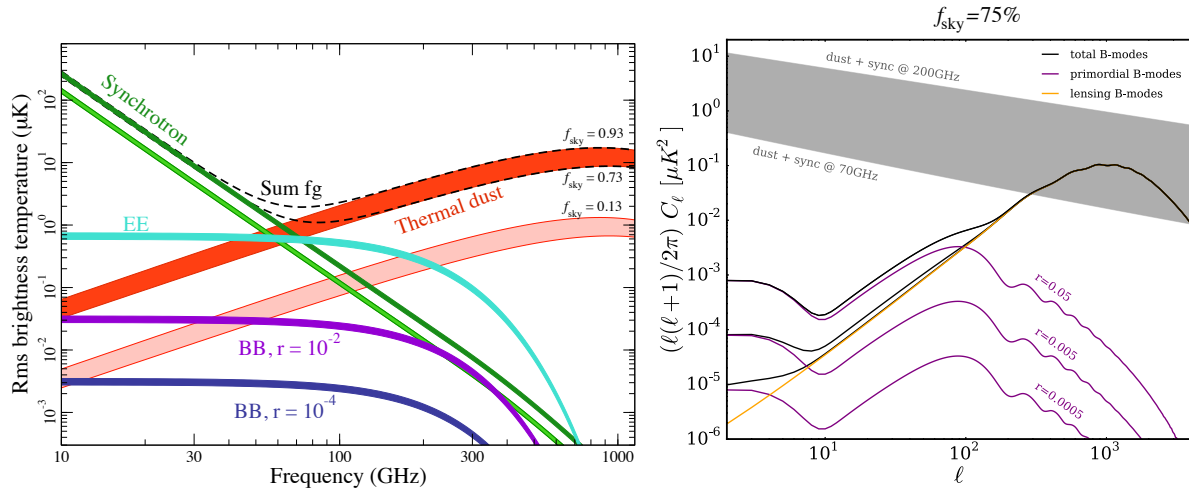
Figure 6: *Left panel:* Brightness temperature as function of frequency for the CMB as well as synchrotron emission (green) and dust emission (red). The darker bands show the brightness temperature for sky fractions between 73% and 93%, the lighter bands show the brightness temperature for the cleanest 13% with the width indicating the uncertainty. *Right panel:* Angular power spectrum for B-mode polarization of the CMB for $r = 0.0005$, $r = 0.005$, and $r = 0.05$ as well as for foreground emission between 70 and 200 GHz.

quired to achieve the science goals. Consequently, optimizing frequency coverage in light of the new information from *Planck* and its limitations will be one of key task of the study proposed here.

To achieve these goals we plan to investigate the effect on the measurements of r and τ of the presence of foregrounds residuals in the CMB maps (after foreground separation and/or cleaning) including, for example, the properties of the polarized thermal dust emission, specifically the potential spatial variation of its spectral index, hinted at by the observed decorrelation of the dust between 217 GHz and 353GHz Planck channels (**??**), and the study of the breakdown of the modified black body spectrum model. These aspects are better explored with the help of physically motivated models of the foregrounds (**??**) and simulations based on these, using either existing simulation tools and/or implementing new simulators when required.

The optimization of frequency channels will be conducted using both traditional (Fisher codes both spectra and map based) and novel techniques currently in development (such as direct Bayesian MCMC inference of cosmological parameters in the presence of foregrounds, (extension of the method presented in **??**). Realistic simulations (including time domain based) are essential to fully assess the performance of a given instrument design/concept in view of both foreground residuals and the presence of systematics. We plan to generate these simulations, process them as we would do the real data, specifically applying some of the current component separation methods to clean the frequency maps from foreground emission (akin to *Planck* collaboration procedures **??**) and propagate to parameter estimation, assessing the impact of all contaminating effects on the accuracy and potential biases of the parameters estimated with particular emphasis on r and τ.

1.3.2 Systematic Errors

Advances in detector technology since the formulation of Planck and WMAP will enable huge gains in raw sensitivity for a CMB probe. To fully take advantage of this sensitivity, system-

atic errors must be controlled to detect polarization signals at nano-Kelvin levels. The proposed study will invest heavily in designing an instrument, test plan, and observation strategy to address systematic errors, gathering decades of experience of ground-, balloon-, and space-based CMB polarimetry. The latest analyses of Planck HFI and LFI data in particular show the effects likely to be important to a future space mission(https://arxiv.org/abs/1605.02985). These systematic errors can be considered in three broad categrories: 1. Intensity-to-polarization leakage, 2. stability, and 3. straylight. Each of these is considered in light of differential polarimetery; the instantaneous signals measured by polarization-sensitive detectors at different times and orientations are combined to recover the maximum likelihood polarization signal from each point on the sky.

Leakage. The CMB temperature signal is many orders of magnitude larger than the polarization B-mode signal (see, e.g. Fig. 1). Therefore, instrumental mismatch effects that can leak even a very small fraction of an intensity fluctuation into a spurious polarization signal must be addressed. The main effects are relative gain and bandpass calibration, differential pointing error, and differential beam shapes.

Relative calibration requirements are likely to exceed those of Planck, whose High Frequency Instrument achieved of order 0.01% (cite https://arxiv.org/abs/1605.02985). Bandpass mismatch is the imperfect matching of the frequency dependant gain of the two detectors or acquisition channels used to estimate the polarized signal. Any asymmetry turns into a spurious polarization signal when viewing sources with SED different from the calibrator. For CMB-probe, this includes every foreground contaminant on the sky. The effect can be minimized by matching the bandpasses, and residual mismatch can be estimated by measuring the bandpasses on the ground, however, for both instruments of Planck the ground based measurements of the bandpasses were found to be insufficient to determine the impact on the polarized maps. In both cases estimates of the bandpass mismatch needed to be determined as part of the mapmaking pipeline, and bandpass mismatch remains one of the most problematic systematics in the pipelines. CMB-probe will need a more robust program to mitigate this problem on ground, simulate the impact, and to deal with it in the flight data.

A second order complication of unmatched bandpasses is unmatched far sidelobe contamination, leading to a spurious polarized component from bright unpolarized signals far from the main lobe.

These systematics are likely to drive the instrumental requirements on the optical system as well as the uniformity of the bandpass of each polarimeter. Calibration requirements will also be set by limiting these systematics: particularly on the knowledge of the polarization parameters (such as cross-polar leakage and the angle of polarization sensitivity), as well as measurement of the beam shape (in general a function of the SED of the observed source). These systematic effects can potentially be mitigated by modulation of the sky signal in such a way that allows complete reconstruction of the polarized sky signal using each photometer, for example, using a half-wave plate.

Stability. Given the need to avoid light from the Sun, Earth, and Moon, the full reconstruction of the polarized sky will necessarily involve combination of measurements made at times seperated by months, requiring stability of the response of the instrument on corresponding time scales. This systematic error puts requirements on control of thermal drifts of spacecraft temperatures, to mitigate thermal emissivity changes and thermoelastic deformation of telescope structures. The cryogenic operating temperatures of detectors or reference calibration loads must be controlled adequately as well. Careful design of the scan strategy can shorten the time scales needed for stringent stability, for example Planck's scan strategy traced out great circles which overlapped on

1 minute timescales, giving a shorter effective time scale for stability requirements.

Additionally, the space radiation environment is modulated by the solar activity and can introduce drifts in the cryogenic thermal environment as well as introducing correlated transients in detectors and readout electronics. The design of the instrument must account this environment, which following Planck is much better understood.

Straylight. The brightest cm-wave and mm-wave sources in the sky (such as the Sun, Moon, planets, and Galactic center) passing into the far sidelobes of the telescope (defined as the response of a detector from a source more than a few degrees from the optical axis) in a sky-synchronous way can create a spurious polarization signal. he far sidelobe response can be reduced by the optical design and baffling, but will always be present at a non-trivial level. The Planck experience is instructive here as well. The detailed GRASP model of the telescope, convolved with the sky model, predicted sidelobe contamination at a visible (10's of microK) level in the 30 GHz maps, which was observed in difference maps. As a result the LFI maps have had an estimate of the sidelobe contamination removed from the timelines as part of the mapmaking process. The more stringent requirements for CMB-probe will necessitate at least this level of mitigation. A major limitation to the analysis of far sidelobe contamination in the Planck data has been the lack of bright enough on-orbit sources to validate the GRASP simlation as adjusted by optical and bandpass parameters estimated on-orbit. Finding a way to better validate the FSL model on-orbit for CMB-probe may be critical to successfully removing FSL contamination.

1.4   Current and Forthcoming Efforts and the CMB Probe

2.5 pages. S3 experiments, forthcoming S4, Baselines CMB Probe options and their complementarity with S4.

Bill Jones is writing this. Due by Oct. 28

1.5   State of Technologies

2 pages. Discuss the technologies, their TRL, and what will be studied

A fourth generation CMB satellite targeting a map sensitivity of $\sim 1\mu\text{k} - \text{arcmin}$ will require, extremely sensitive detector arrays, tight control over systematics, and ability to reject polarized foregrounds as is described in Section 1.2. Given the frequency dependance of synchrotron and dust foregrounds, this last requirement translates into the need for a large number of spectral bands covering the approximate frequency range from ~ 30 GHz to ~ 800 GHz. Development of the CMB technologies needed to meet these requirements is actively being pursued by many groups who are also demonstrating these technologies on ground, balloon, and satellite platforms. We describe the status and needs in the areas of telescopes, optics, detector coupling, detectors, and readout.

Telescopes: Carbon Fiber Reinforced Polymer (CFRP) mirrors are at TRL 9 as they have flown on the Planck sattelite. Their 1.9x1.5 m mirror weighted only 28 lbs and met all surface quality requirements. However, small deformations in the mirror caused by its structural supports had a measurable impact to the beam far-sidelobes that was not caputred by preflight measurements or the corresponding beam modeling. Future CMB satellites will require improved pre-flight characterization of *polarized beam* at operating temperature augmented by improved simulation tools to meet even more systematics requirements. Current ground and balloon born optical designs achieve large field of views (FOVs) with reflective and refractive designs; related designs and their implementation should studied in the context of a satellite mission as the sensitivity requirements

lead to the need to maximize the size of the FOV while fitting within the tight mass and size constraints imposed by a space mission. Given the heritage of past satellite missions it will be possible to develop a telescope design that meets the requirements for a future mission and uses high TRL components.

Optical Coupling: The need for sensitivity drives the push for high efficiency optics; wide bandwidth to compliment mutichroic detector ; infrared filters to maximize cryogenic performance; and polarization modulators to suppress $1/f$ noise and mitigate instrument systematics. The CMB field has made tremendous progress recently by drawing on advances in materials, processing techniques, and developments in electrical engineering including meta-material research. Single crystals such as silicon and sapphire are attractive since they offer extremely low dielectric losses and high indices of refraction to better manipulate light. New coating techniques have been developed for silicon and sapphire that span 2:1 bandwidth (TRL 5+ for silicon) and can realize up to 5:1 bandwidth. EBEX deployed broadband cryogenic polarization modulator with a superconducting bearing that covered 150 GHz band to 410 GHz band raising the modulators to TRL 5+ for space. Meta-material metal-mesh optical filters were deployed with the Planck satellite and they are extensively used by ground based and balloon experiments making these TRL6 optical elements. It is necessary to develop a plan for a satellite mission that will cover ~ 30 GHz to ~ 800 GHz. Two configurations could be considered: multiple optical paths with $< 3 : 1$ bandwidth and a potentially simpler design with only two optical paths with $\sim 5 : 1$ bandwidth. These studies include evaluating the design tradeoffs inherent to these approaches, developing the new coatings needed, and evaluating the promise of hybrid approaches where filters and lenses are implemented in the same optical elements. In addition, the cryogenic rotation mechanism should be demonstrated at the robustness (eg lifetime) needed for for a satellite mission.

Detector Coupling: The focal-plane feed determines the shape and polarization properties of the pixel beams and therefore plays a strong role in controlling systematic errors. The feed design also can determine the total bandwidth and number of photometric bands of each pixel which is important for the efficient use of a telescope's focal plane area. CMB experiments developed broadband multi-chroic *detector* to increase optical throughput of a focal plane. Broadband feed captures signal over wide frequency range. Then on-chip superconducting filter partitions signal into multiple frequency bands prior to detection. Broadband detectors were realized with spline profiled horn and lenslet coupled antenna. Broadband horn detector deployed a pixel that covers 2.3:1 bandwidth with on going development for extending bandwidth to 6:1. Broadband lenslet coupled antenna will deploy 3:1 bandwidth detector this year. Lenslet coupled antenna demonstrated 5:1 bandwidth in laboratory. RF-techniques to partition broadband signals into multiple band are mature. For a future CMB polarization satellite mission, broadband feed should be demonstrated at high frequency where alignment and line width for micro-fabrication becomes challenging. Detectors for CMB satellite mission were hand picked one by one for optimal performance. Next generation of detector array will be fabricated on a silicon wafer. Micro-fabrication process should demonstrate high yield and uniformity across a wafer that can meet tight requirement of satellite mission. Also detector test need to able to characterize detector beyond the level of systematic required by next generation CMB satellite experiment.

The Planck HFI deployed Neutron Transmutation Doped Germanium high-resistance bolometer at 100 milli-Kelvin to achieve photon noise limited detector performance. A Transition Edge

Sensor (TES) bolometer uses a steep transition of superconducting metal to improve linearity of the detector. TES bolometers have been deployed on 100 milli-Kelvin and 250 milli-Kelvin platform. TES bolometers have been deployed across ground based and balloon CMB experiments spanning 40 GHz-410 GHz with detectors achieving NEPs of 20-50 aW/$\sqrt{\text{Hz}}$, nearly background limited at CMB frequencies. TES bolometers deployed at low optical frequencies ($\sim$40 GHz) and balloon-borne payloads should realized even lower NEPs of $\sim$10 aW/$\sqrt{\text{Hz}}$. Emerging detector technology for CMB experiment is kinetic-inductance detector (KIDs). The KIDs detector detects signal as change in kinetic inductance. KIDs detectors can be frequency multiplexed easily to $\sim 1,000$ detectors. Recently, on-sky demonstration at 150 GHz and 230 GHz was done with lumped element KID detector. Noise performance of KID detector at low frequency channels (< 40 GHz) need some improvement to be photon-noise limited. Currently there is no CMB polarizatin power spectrum data produced with KID detector. Coupling between RF (100 GHz) signal to micro-wave KID (MKID) detector is in a development stage. Planck detectors experienced unexpectedly high rate of cosmic ray events. Data was successfully cleaned with analysis technique. Study of impact of cosmic rays on a detector is crucial for next CMB satellite mission.

Multiplexed readout is being used by CMB experiments to readout thousands of TES bolometers, and readout multiplexing is built into KID detector architecture. Voltage bias and low impedance of a TES bolometer facilitates multiplexing readout by Superconducting Quantum Interference Device (SQUID). Time domain multiplexing uses a SQUID at milli-Kelvin as a switch to rapidly cycle through bolometers. Highest achieved multiplexing factor is 64 channels. Frequency domain multiplexing uses superconducting resonators to assign bolometers to different frequency channels. Highest achieved multiplexing factor is 68 channels. New readout scheme, such as microwave SQUID readout, is emerging to increase multiplexing factor for TES bolometer. MKID detector architecture has multiple resonators coming off from a transmission line. A resonator is both a detector and multiplexer. MKID demonstrated multiplexing factor that exceeds 1,000 channels. For next generation satellite experiment that will readout over thousands detectors require high multiplexing factor. Multiplexing factor is directly related to readout complexity and power consumption. Also the Planck mission experienced ADC non-linearity, thus extensive characterization of end to end readout archtecture should be performed pre-flight.

A future CMB satellite mission offers exciting opportunity for millimeter wave polarization science. Experience from Planck mission will be studied to learn lessons for the future mission. Development for CMB instrumentation is an active field with many institutions developing new technologies for ground based, balloon, and proposed satellite missions. For a satellite instrumentation, there is a difficult trade off between desire to have high performance instrument and desire to keep cost manageable. Many developments that is going on for ground based and balloon experiment have similar goal as satellite mission that collaborative development across all platform will be beneficial.

1.6 Mission Study, and Management Plan

1.5 pages; Describe what we want to do, who is doing what, what we are funding

Shaul is writing this. Due by Tuesday Nov. 1

References

[1] J. C. Mather, E. S. Cheng, D. A. Cottingham, R. E. Eplee, Jr., D. J. Fixsen, T. Hewagama, R. B. Isaacman, K. A. Jensen, S. S. Meyer, P. D. Noerdlinger, S. M. Read, and L. P. Rosen. Measurement of the cosmic microwave background spectrum by the COBE FIRAS instrument. *Ap. J.*, 420:439–444, January 1994.

[2] D. J. Fixsen, E. S. Cheng, J. M. Gales, J. C. Mather, R. A. Shafer, and E. L. Wright. The Cosmic Microwave Background Spectrum from the Full COBE FIRAS Data Set. *Ap. J.*, 473:576–+, December 1996.

[3] Y. B. Zeldovich and R. A. Sunyaev. The Interaction of Matter and Radiation in a Hot-Model Universe. *ApSS*, 4:301–316, July 1969.

[4] R. A. Sunyaev and Y. B. Zeldovich. The interaction of matter and radiation in the hot model of the Universe, II. *ApSS*, 7:20–30, April 1970.

[5] R. Keisler, C. L. Reichardt, K. A. Aird, B. A. Benson, L. E. Bleem, J. E. Carlstrom, C. L. Chang, H. M. Cho, T. M. Crawford, A. T. Crites, T. de Haan, M. A. Dobbs, J. Dudley, and E. M. George. A Measurement of the Damping Tail of the Cosmic Microwave Background Power Spectrum with the South Pole Telescope. *Ap. J.*, 743:28, December 2011.

[6] http://bolo.berkeley.edu/polarbear/.

[7] A. H. Guth. Inflationary universe: A possible solution to the horizon and flatness problems. *Phys. Rev. D.*, 23:347–356, January 1981.

[8] A. D. Linde. A New Inflationary Universe Scenario: A Possible Solution of the Horizon, Flatness, Homogeneity, Isotropy and Primordial Monopole Problems. *Phys. Lett.*, B108:389–393, 1982.

[9] A. Albrecht and P. J. Steinhardt. Cosmology for grand unified theories with radiatively induced symmetry breaking. *Phys. Rev. Lett.*, 48:1220–1223, 1982.

[10] K. Sato. First-order phase transition of a vacuum and the expansion of the Universe. *MNRAS*, 195:467–479, May 1981.

[11] E. W. Kolb and M. S. Turner. *The Early Universe*. Addison-Wesley, Redwood City, CA, 2nd. edition, 1994.

[12] M. Kamionkowski, A. Kosowsky, and A. Stebbins. A Probe of Primordial Gravity Waves and Vorticity. *Phys. Rev. Lett.*, 78:2058–2061, March 1997. astro-ph/9609132.

[13] M. Zaldarriaga and U. Seljak. All-sky analysis of polarization in the microwave background. *Phys. Rev. D.*, 55:1830–1840, 1997.

[14] Hayden Lee, S. C. Su, and Daniel Baumann. The Superhorizon Test of Future B-mode Experiments. *JCAP*, 1502(02):036, 2015.

[15] David H. Lyth. What would we learn by detecting a gravitational wave signal in the cosmic microwave background anisotropy? *Phys.Rev.Lett.*, 78:1861–1863, 1997.

[16] Ryo Namba, Marco Peloso, Maresuke Shiraishi, Lorenzo Sorbo, and Caner Unal. Scale-dependent gravitational waves from a rolling axion. *JCAP*, 1601(01):041, 2016.

[17] Marco Peloso, Lorenzo Sorbo, and Caner Unal. Rolling axions during inflation: perturbativity and signatures. 2016.

[18] R. A. Sunyaev and Y. B. Zeldovich. Small scale entropy and adiabatic density perturbations - Antimatter in the Universe. *ApSS*, 9:368–382, December 1970.

[19] R. A. Daly. Spectral distortions of the microwave background radiation resulting from the damping of pressure waves. *Ap. J.*, 371:14–28, April 1991.

[20] W. Hu, D. Scott, and J. Silk. Power spectrum constraints from spectral distortions in the cosmic microwave background. *Ap. J. Lett.*, 430:L5–L8, July 1994.

[21] J. Chluba, R. Khatri, and R. A. Sunyaev. CMB at 2 x 2 order: the dissipation of primordial acoustic waves and the observable part of the associated energy release. *MNRAS*, 425:1129–1169, September 2012.

[22] J. Chluba. Which spectral distortions does ΛCDM actually predict? *MNRAS*, 460:227–239, July 2016.

[23] J. Chluba, A. L. Erickcek, and I. Ben-Dayan. Probing the Inflaton: Small-scale Power Spectrum Constraints from Measurements of the Cosmic Microwave Background Energy Spectrum. *Ap. J.*, 758:76, October 2012.

[24] J. B. Dent, D. A. Easson, and H. Tashiro. Cosmological constraints from CMB distortion. *Phys. Rev. D.*, 86(2):023514, July 2012.

[25] J. Chluba and D. Jeong. Teasing bits of information out of the CMB energy spectrum. *MNRAS*, 438:2065–2082, March 2014.

[26] S. Clesse, B. Garbrecht, and Y. Zhu. Testing inflation and curvaton scenarios with CMB distortions. *JCAP*, 10:046, October 2014.

[27] G. Cabass, A. Melchiorri, and E. Pajer. μ distortions or running: A guaranteed discovery from CMB spectrometry. *Phys. Rev. D.*, 93(8):083515, April 2016.

[28] E. Pajer and M. Zaldarriaga. New Window on Primordial Non-Gaussianity. *Physical Review Letters*, 109(2):021302, July 2012.

[29] J. Ganc and E. Komatsu. Scale-dependent bias of galaxies and μ-type distortion of the cosmic microwave background spectrum from single-field inflation with a modified initial state. *Phys. Rev. D.*, 86(2):023518, July 2012.

[30] M. Biagetti, H. Perrier, A. Riotto, and V. Desjacques. Testing the running of non-Gaussianity through the CMB μ-distortion and the halo bias. *Phys. Rev. D.*, 87(6):063521, March 2013.

[31] R. Emami, E. Dimastrogiovanni, J. Chluba, and M. Kamionkowski. Probing the scale dependence of non-Gaussianity with spectral distortions of the cosmic microwave background. *Phys. Rev. D.*, 91(12):123531, June 2015.

[32] J. Chluba, E. Dimastrogiovanni, M. A. Amin, and M. Kamionkowski. Evolution of CMB spectral distortion anisotropies and tests of primordial non-Gaussianity. *ArXiv e-prints*, October 2016.

[33] R. A. Sunyaev and J. Chluba. Signals from the epoch of cosmological recombination (Karl Schwarzschild Award Lecture 2008). *Astronomische Nachrichten*, 330:657–+, 2009.

[34] J. Chluba and Y. Ali-Haïmoud. COSMOSPEC: fast and detailed computation of the cosmological recombination radiation from hydrogen and helium. *MNRAS*, 456:3494–3508, March 2016.

[35] Christopher Brust, David E. Kaplan, and Matthew T. Walters. New Light Species and the CMB. *JHEP*, 12:058, 2013.

[36] Daniel Baumann, Daniel Green, and Benjamin Wallisch. A New Target for Cosmic Axion Searches. *Phys. Rev. Lett.*, 117(17):171301, 2016.

[37] Sergei Bashinsky and Uros Seljak. Neutrino perturbations in CMB anisotropy and matter clustering. *Phys. Rev.*, D69:083002, 2004.

[38] Zhen Hou, Ryan Keisler, Lloyd Knox, Marius Millea, and Christian Reichardt. How Massless Neutrinos Affect the Cosmic Microwave Background Damping Tail. *Phys. Rev.*, D87:083008, 2013.

[39] Brent Follin, Lloyd Knox, Marius Millea, and Zhen Pan. First Detection of the Acoustic Oscillation Phase Shift Expected from the Cosmic Neutrino Background. *Phys. Rev. Lett.*, 115(9):091301, 2015.

[40] Daniel Baumann, Daniel Green, Joel Meyers, and Benjamin Wallisch. Phases of New Physics in the CMB. *JCAP*, 1601:007, 2016.

[41] Daniel Green, Joel Meyers, and Alexander van Engelen. CMB Delensing Beyond the B Modes. 2016.

[42] Willy Fischler and Joel Meyers. Dark Radiation Emerging After Big Bang Nucleosynthesis? *Phys. Rev.*, D83:063520, 2011.

[43] S. Sarkar and A. M. Cooper. Cosmological and experimental constraints on the tau neutrino. *Physics Letters B*, 148:347–354, November 1984.

[44] M. Kawasaki and K. Sato. The effect of radiative decay of massive particles on the spectrum of the microwave background radiation. *Physics Letters B*, 169:280–284, March 1986.

[45] W. Hu and J. Silk. Thermalization constraints and spectral distortions for massive unstable relic particles. *Physical Review Letters*, 70:2661–2664, May 1993.

[46] J. Chluba. Distinguishing different scenarios of early energy release with spectral distortions of the cosmic microwave background. *MNRAS*, 436:2232–2243, December 2013.

[47] E. Dimastrogiovanni, L. M. Krauss, and J. Chluba. Constraints on gravitino decay and the scale of inflation using CMB spectral distortions. *Phys. Rev. D.*, 94(2):023518, July 2016.

[48] X. Chen and M. Kamionkowski. Particle decays during the cosmic dark ages. *Phys. Rev. D.*, 70(4):043502–+, August 2004.

[49] L. Zhang, X. Chen, M. Kamionkowski, Z.-G. Si, and Z. Zheng. Constraints on radiative dark-matter decay from the cosmic microwave background. *Phys. Rev. D.*, 76(6):061301–+, September 2007.

[50] R. Diamanti, L. Lopez-Honorez, O. Mena, S. Palomares-Ruiz, and A. C. Vincent. Constraining dark matter late-time energy injection: decays and p-wave annihilations. *JCAP*, 2:017, February 2014.

[51] M. Kawasaki, K. Kohri, and T. Moroi. Big-bang nucleosynthesis and hadronic decay of long-lived massive particles. *Phys. Rev. D.*, 71(8):083502, April 2005.

[52] M. Kawasaki, K. Kohri, and T. Moroi. Hadronic decay of late-decaying particles and big-bang nucleosynthesis. *Physics Letters B*, 625:7–12, October 2005.

[53] K. Jedamzik. Big bang nucleosynthesis constraints on hadronically and electromagnetically decaying relic neutral particles. *Phys. Rev. D.*, 74(10):103509, November 2006.

[54] J. Chluba and R. A. Sunyaev. The evolution of CMB spectral distortions in the early Universe. *MNRAS*, 419:1294–1314, January 2012.

[55] K. Jedamzik, V. Katalinić, and A. V. Olinto. Limit on Primordial Small-Scale Magnetic Fields from Cosmic Microwave Background Distortions. *PRL*, 85:700–703, July 2000.

[56] H. Tashiro, E. Sabancilar, and T. Vachaspati. CMB distortions from superconducting cosmic strings. *Phys. Rev. D.*, 85(10):103522, May 2012.

[57] A. D. Dolgov and D. Ejlli. Resonant high energy graviton to photon conversion at the post-recombination epoch. *Phys. Rev. D.*, 87(10):104007, May 2013.

[58] H. Tashiro, J. Silk, and D. J. E. Marsh. Constraints on primordial magnetic fields from CMB distortions in the axiverse. *Phys. Rev. D.*, 88(12):125024, December 2013.

[59] R. R. Caldwell and N. A. Maksimova. Spectral distortion in a radially inhomogeneous cosmology. *Phys. Rev. D.*, 88(10):103502, November 2013.

[60] P. J. E. Peebles, S. Seager, and W. Hu. Delayed Recombination. *Ap. J. Lett.*, 539:L1–L4, August 2000.

[61] N. Padmanabhan and D. P. Finkbeiner. Detecting dark matter annihilation with CMB polarization: Signatures and experimental prospects. *Phys. Rev. D.*, 72(2):023508–+, July 2005.

[62] Tracy R. Slatyer and Chih-Liang Wu. General Constraints on Dark Matter Decay from the Cosmic Microwave Background. 2016.

[63] Cora Dvorkin, Kfir Blum, and Marc Kamionkowski. Constraining Dark Matter-Baryon Scattering with Linear Cosmology. *Phys. Rev.*, D89(2):023519, 2014.

[64] Francis-Yan Cyr-Racine, Roland de Putter, Alvise Raccanelli, and Kris Sigurdson. Constraints on Large-Scale Dark Acoustic Oscillations from Cosmology. *Phys. Rev.*, D89(6):063517, 2014.

[65] Manuel A. Buen-Abad, Gustavo Marques-Tavares, and Martin Schmaltz. Non-Abelian dark matter and dark radiation. *Phys. Rev.*, D92(2):023531, 2015.

[66] Julien Lesgourgues, Gustavo Marques-Tavares, and Martin Schmaltz. Evidence for dark matter interactions in cosmological precision data? *JCAP*, 1602(02):037, 2016.

[67] Y. Ali-Haïmoud, J. Chluba, and M. Kamionkowski. Constraints on Dark Matter Interactions with Standard Model Particles from Cosmic Microwave Background Spectral Distortions. *Physical Review Letters*, 115(7):071304, August 2015.

[68] R. Essig, A. Manalaysay, J. Mardon, P. Sorensen, and T. Volansky. First Direct Detection Limits on Sub-GeV Dark Matter from XENON10. *Physical Review Letters*, 109(2):021301, July 2012.

[69] C. Bœhm, J. A. Schewtschenko, R. J. Wilkinson, C. M. Baugh, and S. Pascoli. Using the Milky Way satellites to study interactions between cold dark matter and radiation. *MNRAS*, 445:L31–L35, November 2014.

[70] Manoj Kaplinghat, Lloyd Knox, and Yong-Seon Song. Determining neutrino mass from the CMB alone. *Phys. Rev. Lett.*, 91:241301, 2003.

[71] J. S. Dunlop. The Cosmic History of Star Formation. *Science*, 333:178, July 2011.

[72] Planck Collaboration, R. Adam, P. A. R. Ade, N. Aghanim, M. Arnaud, J. Aumont, C. Baccigalupi, A. J. Banday, R. B. Barreiro, J. G. Bartlett, and et al. Planck intermediate results. XXX. The angular power spectrum of polarized dust emission at intermediate and high Galactic latitudes. *ArXiv e-prints*, September 2014.

[73] Planck Collaboration, P. A. R. Ade, N. Aghanim, C. Armitage-Caplan, M. Arnaud, M. Ashdown, F. Atrio-Barandela, J. Aumont, C. Baccigalupi, A. J. Banday, and et al. Planck 2013 results. XVIII. The gravitational lensing-infrared background correlation. *Astron. Astrophys.*, 571:A18, November 2014.

[74] P. Madau and M. Dickinson. Cosmic Star-Formation History. *ARA&A*, 52:415–486, August 2014.

[75] P. Serra, G. Lagache, O. Doré, A. Pullen, and M. White. Cross-correlation of cosmic far-infrared background anisotropies with large scale structures. *Astron. Astrophys.*, 570:A98, October 2014.

[76] L. Wang, M. Viero, N. P. Ross, V. Asboth, M. Béthermin, J. Bock, D. Clements, A. Conley, A. Cooray, D. Farrah, A. Hajian, J. Han, G. Lagache, G. Marsden, A. Myers, P. Norberg, S. Oliver, M. Page, M. Symeonidis, B. Schulz, W. Wang, and M. Zemcov. Co-evolution of black hole growth and star formation from a cross-correlation analysis between quasars and the cosmic infrared background. *MNRAS*, 449:4476–4493, June 2015.

[77] C. Feng, A. Cooray, and B. Keating. Planck Lensing and Cosmic Infrared Background Cross-Correlation with Fermi-LAT: Tracing Dark Matter Signals in the γ-ray Background. *ArXiv e-prints*, August 2016.

[78] R. A. Sunyaev and Y. B. Zeldovich. Formation of Clusters of Galaxies; Protocluster Fragmentation and Intergalactic Gas Heating. *Astron. Astrophys.*, 20:189–+, August 1972.

[79] W. Hu, D. Scott, and J. Silk. Reionization and cosmic microwave background distortions: A complete treatment of second-order Compton scattering. *Phys. Rev. D.*, 49:648–670, January 1994.

[80] S. P. Oh, A. Cooray, and M. Kamionkowski. Sunyaev-Zeldovich fluctuations from the first stars? *MNRAS*, 342:L20–L24, June 2003.

[81] R. Cen and J. P. Ostriker. Where Are the Baryons? *Ap. J.*, 514:1–6, March 1999.

[82] A. Refregier, E. Komatsu, D. N. Spergel, and U.-L. Pen. Power spectrum of the Sunyaev-Zel'dovich effect. *Phys. Rev. D.*, 61(12):123001, June 2000.

[83] J. C. Hill, N. Battaglia, J. Chluba, S. Ferraro, E. Schaan, and D. N. Spergel. Taking the Universe's Temperature with Spectral Distortions of the Cosmic Microwave Background. *Physical Review Letters*, 115(26):261301, December 2015.

[84] Planck Collaboration, P. A. R. Ade, N. Aghanim, C. Armitage-Caplan, M. Arnaud, M. Ashdown, F. Atrio-Barandela, J. Aumont, C. Baccigalupi, A. J. Banday, and et al. Planck 2013 results. XX. Cosmology from Sunyaev-Zeldovich cluster counts. *Astron. Astrophys.*, 571:A20, November 2014.

[85] S. Y. Sazonov and R. A. Sunyaev. Cosmic Microwave Background Radiation in the Direction of a Moving Cluster of Galaxies with Hot Gas: Relativistic Corrections. *Ap. J.*, 508:1–5, November 1998.

[86] N. Itoh, Y. Kohyama, and S. Nozawa. Relativistic corrections to the sunyaev-zeldovich effect for clusters of galaxies. *Ap. J.*, 502:7, July 1998.

[87] A. Challinor and A. Lasenby. Relativistic corrections to the sunyaev-zeldovich effect. *Ap. J.*, 499:1, May 1998.

[88] J. A. Rubiño-Martín, C. Hernández-Monteagudo, and R. A. Sunyaev. The imprint of cosmological hydrogen recombination lines on the power spectrum of the CMB. *Astron. Astrophys.*, 438:461–473, August 2005.

[89] C. Hernández-Monteagudo, J. A. Rubiño-Martín, and R. A. Sunyaev. On the influence of resonant scattering on cosmic microwave background polarization anisotropies. *MNRAS*, 380:1656–1668, October 2007.

[90] A. Lewis. Rayleigh scattering: blue sky thinking for future CMB observations. *JCAP*, 8:053, August 2013.

[91] K. Basu, C. Hernández-Monteagudo, and R. A. Sunyaev. CMB observations and the production of chemical elements at the end of the dark ages. *Astron. Astrophys.*, 416:447–466, March 2004.

[92] D. R. G. Schleicher, D. Galli, F. Palla, M. Camenzind, R. S. Klessen, M. Bartelmann, and S. C. O. Glover. Effects of primordial chemistry on the cosmic microwave background. *Astron. Astrophys.*, 490:521–535, November 2008.

2 Curriculum Vitae

3 Summary of Work Effort

4 Current and Pending Support

5   Letters of Support

6 Budget Details - Narrative

6.1 Team, and Work Effort

6.1.1 Funded Team Members

6.1.2 Non-Funded Team Members

6.2 Costing Principles

- **Summer Salaries:**
  - **Workshop:**

6.3 University of Minnesota Budget

6.3.1 Direct Labor

6.3.2 Supplies

6.3.3 Travel

6.3.4 Other Direct Costs

Publications and Teleconferencing
   Other Subcontracts

6.3.5 Facilities and Administrative Costs

7   Budget Sheets

ACS attitude control system

ADC analog-to-digital converters

ADS attitude determination software

AHWP achromatic half-wave plate

AMC Advanced Motion Controls

ARC anti-reflection coatings

ATA advanced technology attachment

BRC bolometer readout crates

BLAST Balloon-borne Large-Aperture Submillimeter Telescope

CANbus controller area network bus

CMB cosmic microwave background

CMM coordinate measurement machine

CSBF Columbia Scientific Balloon Facility

CCD charge coupled device

DAC digital-to-analog converters

DASI Degree Angular Scale Interferometer

dGPS differential global positioning system

DfMUX digital frequency domain multiplexer

DLFOV diffraction limited field of view

DSP digital signal processing

EBEX E and B Experiment

EBEX2013 EBEX2013

ELIS EBEX low inductance striplines

ETC EBEX test cryostat

FDM frequency domain multiplexing

FPGA field programmable gate array

FCP flight control program

FOV field of view

FWHM full width half maximum

GPS global positioning system

HDPE high density polyethylene

HIM high index materials

HWP half-wave plate

IA integrated attitude

IP instrumental polarization

JSON JavaScript Object Notation

LDB long duration balloon

LED light emitting diode

LCS liquid cooling system

LC inductor and capacitor

LZH Lazer Zentrum Hannover

MCP multi-color pixel

MSM millimeter and sub-millimeter

MLR multilayer reflective

MAXIMA Millimeter Anisotropy eXperiment IMaging Array

NASA National Aeronautics and Space Administration

NDF neutral density filter

PCB printed circuit board

PE polyethylene

PME polarization modulation efficiency

PSF point spread function

PV pressure vessel

PWM pulse width modulation

RMS root mean square

SLR single layer reflective

SMB superconducting magnetic bearing

SQUID superconducting quantum interference device

SQL structured query language

STARS star tracking attitude reconstruction software

SWS sub-wavelength structures

TES transition edge sensor

TDRSS tracking and data relay satellites

TM transformation matrix

UHMWPE ultra high molecular weight polyethylene

UMN University of Minnesota